3D-printing methacrylate/chitin nanowhiskers composites via stereolithography: Mechanical and thermal properties

Reymark D. Maalihan[a,b,c], Bryan B. Pajarito[a], Rigoberto C. Advincula[c]

[a]Polymer Research Laboratory, Department of Chemical Engineering, University of the Philippines Diliman. Quezon City 1101. Philippines
[B]Chemical and Food Engineering Department, Batangas State University, Batangas City 4200, Philippines
[C]Department of Macromolecular Science and Engineering, Case Western Reserve University, OH 44106, USA

Abstract

We report on the mechanical and thermal properties of stereolithography (SI.A) JD-printed methacrylate (MA) resin reinforced by chitin nanowhiskers (CNWs). CNWs were synthesized by acid hydrolysis of crab shell chitin and nanocomposites with 0 wt%, 0.5 wt%, 1.0 wt %, and 1.5 wt % CNWs loading were prepared by slurry compounding method. The obtained CNWs (diameter= 23 ± 5 nm, length= 253 ± 100 nm, and aspect ratio = 11 ± 3) are well dispersed within the bulk of MA at 1.0 wt % loading, implying good interfacial adhesion between the nanofiller and the resin matrix possibly due to hydrogen bonding interactions. The addition of up to 1.0 wt% CNWs to neat MA enhances the tensile strength, strain at break, modulus, and maximum thermal degradation temperatures of the nanocomposites. Moreover, the incorporation of CNWs not only improves the mechanical and thermal properties, but also preserves the excellent resolution and accuracy of JD-printed MA/CNWs nanocomposites.

Keywords

3D-printing; Stereolithography; Chitin nanowhisker; Methacrylate; Slurry compounding; Nanocomposites

Acknowledgements

The authors acknowledge the Department of Science and Technology (Philippines), through the Engineering Research and Development for Technology for the research dissemination grant and the Swagelok Center for Surface Analysis of Materials (Case Western Reserve University, USA) for TEM analysis and high- resolution optical microscopy.

Introduction

Three-dimensional (3D)-printing is a revolutionary manufacturing process that transforms the way materials are fabricated into functional products. It involves adding and joining materials to form a part in a layer-by-layer fashion, hence additive manufacturing [1-3]. Compared with traditional subtractive manufacturing methods, 3D-printing offers a higher degree of automation and more accurate production of complex architectures without the use of molds and cutting tools [4-7]. Among various 3D-printing technologies, stereolithography (SIA) is considered a powerful and versatile technique due to its high feature resolution, high accuracy, and fast printing time [1,6]. In SIA, a liquid photosensitive resin is exposed locally to ultraviolet laser and is then cured and solidified in layers [2,6]. Methacrylate **(MA)** resins are one of the most used materials for SIA 3D-printing due to their excellent transparency, high modulus, and ease of processing [6,8]. However, applications of MA photopolymers are limited due to their brittleness at small strains and low thermal stability at elevated temperatures [6,9,10]. In this regard, the improvement of overall mechanical and thermal properties of such SIA materials for 3D- printing is necessary.

Recent advances in formulating SIA resins are mainly focused on incorporation of fillers such as inorganic particles [10], graphene oxide [9,11], and cellulose nanocrystals [8,12] into polymer matrix to create 3D- printed composites with enhanced mechanical, thermal, and electrical properties. From a practical standpoint, polysaccharide-based natural fillers have attracted interest in both academia and industry due to their outstanding reinforcement properties, abundance, and renewability [12 ,13]. Thus, novel and creative ways of producing, marketing, and value-adding composites via 3D manufacturing can be realized to develop mechanically robust, environment friendly, and innovative materials. Among the many natural fillers available today, chitin is of great interest in this study not only as underutilized biomass but also as versatile and functional feedstock in 3D-printing. It is the primary structural component of the exoskeleton of crustaceans such as crabs and shrimps which are usually considered as wastes from sea food processing industries [13]. Nanowhiskers, obtained from acid hydrolysis of chitin, have a rod-like morphology with dimensions of ~ 200- 400 nm in length and ~ 20- 30 nm in width. Subsequently, the high aspect ratio (~10-13) and modulus (200 GPa) result to an excellent reinforcing effect of chitin nanowhiskers (CNWs) on different polymer matrices to create high-performance nanocomposites [13,14]. Likewise, the mechanical and thermal characteristics of CNWs-filled nanocomposites are significantly influenced by the successful dispersion of the hydrophilic CNWs into the hydrophobic polymer matrix. Methods such as freeze drying, high-energy ultrasonication, and slurry compounding are done to reduce the surface polarity between the filler and matrix and to avoid the agglomeration of fillers [6,8,15,16]. In this study, we pre- pared CNWs by acid hydrolysis of chitin and were processed with MA resin by slurry compounding to obtain bulk nanocomposites with different loadings of CNWs. The structure of CNWs and the nanocomposites were characterized by Fourier-transform infrared spectroscopy (FTIR) and transmission electron microscopy (TEM). The mechanical and thermal properties of 3D-printed nanocomposites were determined by tensile tests and thermogravimetric analysis (TGA), respectively. Finally, optical microscopy of 3D- printed MA/CNWs nanocomposites were performed to assess the complexity and dimensional accuracy of the fabrication technique.

Experimental

Materials

Methacrylate (MA)-containing photopolymer clear resin (density ~1.1 g/mL) was purchased from Formlabs Inc. (Somerville, MA, USA). Chitin powder from crab shells was purchased from Koyo Chemical Co. Ltd. Uapan). All other chemicals were purchasedfrom Sigma-Aldrich (Milwaukee, WI, USA) and used as received.

Preparation of CNWS

CNWs were prepared from chitin powder based on acid hydrolysis method of Liu et al. [16] with slight modifications. Chitin was hydrolyzed using 3 N HCI (30 ml HCl per g chitin) at 105 °C under agitation for 90 min. Purification was done by successive washing with deionized water, centrifugation (4400 rpm, 15 min), and dialysis (24 h). A further ultrasonic treatment using a Cole-Parmer ultrasonicator (800 W, 1 h) was performed for better dispersion of CNWs in aqueous suspension at nanoscale. Finally, the CNWs suspension was Iyophilized for further use.

Preparation of MA/CNWs nanocomposites for 3D-printing

MA/CNWs nanocomposites with 0, 0.5, 1.0, and 1.5 wt% CNWs were prepared via modified slurry compounding technique [15,16]. Pre-determined amounts of MA and CNWs were mixed separately in ethanol by ultrasonication for 15 min. CNWs- ethanol suspension was then added to the MA-ethanol solution to achieve the final desired weight content of CNWs in MA. The resulting solution was mixed magnetically and vacuum-dried at 60 °C to remove the ethanol. The final nanocomposite resin was further ultrasonicated for 10 min to maintain homogeneity prior to

printing. Samples were then printed using a Formlabs (Form 2) SLA 3D-printer with a wavelength of 405 nm and spot size of 140 µm. An optimized setting for printing commercial SLA resin (resolution = 50 µm) was used for 3D-fabrication of nanocomposites.

FTIR spectroscopy

The FTIR spectra were obtained using Agilent Cary 600 Series spectrometer in the ATR mode within 4000- 400 cm^{-1} wave number range. Absorbance values were then normalized and the spectral changes in the functional group region upon addition of CNWswere observed using Origin software.

TEM imaging

The morphology of CNWs and the quality of CNWs dispersion in the nanocomposites were observed under Tecnai TF30 ST trans- mission electron microscope operating at an accelerating voltage of 300 kV. Adrop of 0.01 wt% w/v CNWs suspension was deposited onto carbon-coated grids. To study the dispersion of CNWs in the nanocomposites, MA/CNWs films were sliced to a thickness of 95 nm with an ultramicrotome (Leica), placed on carbon-coated grids, and TEM images were taken.

Tensile testing

Tensile tests were carried out on printed dogbones (70 mm^3 x 4 mm^3 x 2.2 mm^3) using MTS universal testing machine (UTM) with a 5 kN load and a crosshead speed of 50mm/min.

Thermogravimetric analysis (TGA)

TGA measurements of 3D-printed nanocomposites were carried out under nitrogen atmosphere using TA Instruments Q500 at a heating rate of 10 °C/min from 25 °C to 600 °C.

Optical microscopy

3D reconstruction and measurement of the surface of 3D- printed object was performed using Keyence VHX-5000 digital microscope.

Results and Discussion

Preparation of CNWs and MA/CNWs nanocomposites

In this study, we showed a simple approach that takes advantage on the nanoscale structure and dispersion of chitin whiskers to enhance the mechanical and thermal properties of commercial 3D-printed resin produced by SLA, as illustrated in Fig. 1. Inspired by a previous study on epoxy/CNWs nanocomposites [15], a slurry- compounding technique was employed to fabricate MA/CNWs nanocomposites as feedstock for 3D-printing. This approach effectively transfers the dispersion state of CNWs in ethanol into MA matrix by a solvent exchange step, which leads to better dispersion of CNWs and interactions with MA resin. The non-covalent interactions of CNWs with MA, as affirmed in the succeeding sections of the paper, activate the interfacial bonding of the filler with the matrix, which is crucial for achieving optimum reinforcement performance of the resulting nanocomposites.

Structure of CNWs and MA/CNWs nanocomposites

The final mechanical and thermal properties of 3D-printed MA/CNWs nanocomposites are affected by the incorporation of CNWs via layer-by-layer photopolymerization printing using SLA. Thus, FTIR spectroscopy was performed to determine the presence of CNWs with varying loading in MA matrix. The full spectra for pure CNWs and 3D-printed specimens- pure MA (0 wt% CNWs) and MA/CNWs nanocomposites with varying CNWs loading (0.5 wt% to 1.5 wt% CNWs) are shown in Fig. 2(a). The spectrum of neat MA specimen mainly exhibits absorption peaks at ~ 3375 cm^{-1} (-OH stretching), ~ 2953 cm^{-1} (- CH_3 stretching), and ~1704 cm^{-1} (C= O stretching) which are consistent with the peaks of commercial SLAMA res in shown by previous studies [8,9]. The presence of oxygen-containing functional groups in the resin allows interactions with CNWs via hydrogen bonding formation [8,9,12,15,17]. On the other hand, the spectrum of pure CNWs shows characteristic absorption bands at ~3455 cm^{-1} (hydrogen- bonded -OH groups), 3254 cm^{-1} (- NH stretching), ~2953 cm^{-1} (-C H_3 stretching), 1658 cm^{-1} (amide I C= O stretching), and ~1558 cm^{-1} (amide II C= O stretching), which are consistent with the previous reported one [17]. As for MA/CNWs nanocomposites, the corresponding spectra of specimens resemble that of pure MA having increased band intensities at the -OH and C= O regions with increasing CNWs content. This confirms the presence of CNWs molecules in MA and the intensified hydrogen bonding between the hydroxyl and carbonyl groups of CNWs and MA [9,15,17]. On the other hand, TEM

imaging was done to investigate the morphology of the nanocomposites and measure the dimensions of CNWs. As illustrated in Fig. 2(b), a representative image of 1.0 wt % CNWs reveals a homogeneous dispersion of CNWs in the MA matrix, confirming that the slurry compounding technique of transferring CNWs into the MA matrix was effective. The CNWs consist of individual chitin fragments with slender parallelepiped rods having approximate diameter and length of 23 ± 5 nm and 253 ± 100 nm, respectively. This provides an aspect ratio (length/- diameter) of 11 ± 3, which is consistent with previous studies [14,15,17]. Thus, the nanosized features of CNWs indicate their potential applications on reinforcing 3D-printed nanocomposites.

Mechanical properties of MA/CNWs nanocomposites

Tensile tests were conducted to establish the effect of CNWs on the mechanical properties of conventional 3D-printed MA resin. Typical stress-strain curves of neat MA (0 wt % CNWs) and MA/ CNWs nanocomposites are shown Fig. 3(a) and the corresponding mechanical properties are presented in Fig. 3(b). Results reveal that neat MA polymer has a tensile strength of 32 ± 1.5 MPa which improves by 44% upon the addition of up to 1.0 wt% CNWs (46 ± 1.2 MPa). The maximum strain at break is also enhanced by incorporation of CNWs at similar loading (8.4 ± 0.5%), achieving 31% increment compared to neat MA (6.4 ± 0.5%). Consequently, the combined increase in the tensile strength and strain at break improves the tensile toughness which corresponds to the area below the stress-strain curves of the nanocomposites (Fig. 3(a)). These improvements are influenced by enhanced interfacial adhesion between CNWs and MA due to formation of strong hydrogen bonds between them as previously validated by FTIR analysis [9,12,15,17]. The 3D-printed nanocomposites resist the premature fracture via a physical, non-covalent network structure between the filler and the matrix, leading to stronger and tougher materials [12]. However, a further increase of the CNWs content to 1.5 wt% reduce both the tensile strength (36 ± 1.6 MPa) and strain at break (3.6 ± 0.4%) by 22% and 57%, respectively compared to 1.0 wt% loading, which is due to the aggregation of CNWs acting as stress concentrators on the material (8,15) . The tensile modulus also improves by increasing the loading of CNWs as shown in Fig. 3 (b). For instance, the tensile modulus at 1.5 wt% CNWs content (1.4 ± 0.1 GPa) exhibits 75% of increment compared to neat MA (0.8 ± 0.1 GPa). This implies that the intrinsic stiffness of CNWs has a direct impact on the modulus of the fabricated material. It further denotes that the resistance of MA/CNWs nanocomposite against tensile deformation is mainly influenced by matrix-filler interactions provided by the hydrogen-bonded functional groups between MA and CNWs [12,17].

Thermal properties of MA/CNW nanocomposites

TGA measurements were carried out to study the effect of CNWs on the thermal stability and decomposition profile of 3D- printed MA/CNWs nanocomposites. The TGA curves of neat MA and MA/CNWs nanocomposites with different loadings of CNWs are presented in Fig. 4(a). Obviously, both neat MA (0 wt% CNWs) and MA/CNWs nanocomposites have two stages of thermal degradation process with two maximum-rate degradation temperatures (T_{max1} and T_{max2}) plotted in Fig. 4(b). The first step between 280℃ and 375°C is associated with the cleavage of terminal vinyl chain units of methacrylate oligomers. Likewise, the second stage between 375 °c and 480 °c (magnified in Fig. 4a) is attributed to the pyrolysis of polymer backbone of MA chains initiated by C-C bond dissociation [8]. With the addition of up to 1.0 wt% CNWs, the T_{max1} value improves from 360.2 ± 0.3 ℃ to 365.6 ± 0.6 ℃ while the T_{max2} value increases from 453.5 ± 0.5 °C to 463.2 ± 0.8 °C, indicating that CNWs retard the degradation of the nanocomposites. The enhancement in the T_{max} values is due to the highly oriented crystal structure of CNWs that can act as a barrier for diffusion of volatiles from thermal decomposition [8]. However, both the T_{max} values drop to 362.3 ± 0.2 ℃ (T_{max1}) and 461.3 ± 0.3 °C (T_{max2}) with the addition of 1.5 wt% CNWs, due to agglomeration of large chitin crystallites on the matrix surface and weak matrix-filler interactions at higher CNWs loading (15) . The mass residues with yields from 2.0 to 2.5% (Fig. 4(b)) for all loadings at 500 °C to 600 °C could be attributed to CNWs and to aromatic photo initiator contained in the MA resin [18]. Aromatics and other cyclic structures are believed to form char residue when thermally degraded at nitrogen atmosphere [12,18].

Fabrication of MA/CNWs nanocomposites by SLA 3D-printing

Finally, to demonstrate the capability of SLA to fabricate high-resolution, microscale structures, cylindrical micropillars (diameter; 220 µm, height; 420µm from CAD model) were printed with the similar printing condition for dogbone samples used for tensile testing. High-resolution optical microscopy was employed to generate magnified images, perform 3D reconstruction, and measure the dimensions of 3D-printed structures as shown in Fig. S(a,b,c). The printed micropillars of MA/CNWs nanocomposites containing 1.5 wt% CNWs exhibit diameter of 219 ± 4 µm and height of 421 ± 11 µm, which are close to the specified dimensions from CAD model and are within the tolerance limit (±100 µm) set by conventional desktop SIA printers [19]. This means that addition of CNWs in commercial MA resin does not significantly influence the print resolution of obtained pillar structures even at relatively high loading of nanofillers. Thus, we anticipate the potential applications of 3D-printed CNW-filled micropillars in the areas of biological templates, micro-regime heat sinks, and cages and channels for chemical reactions where enhanced thermo-mechanical properties are necessary [20,21]. It is also worth noting that reinforced MA/CNWs nanocomposites can be 3D-fabricated without performing optimization on the set- tings of the 3D-printer. Thus, the compatibility with commercial 3D-printers can

extend the applications of these materials that require excellent mechanical and thermal properties.

Conclusions

In summary, we utilized a simple slurry compounding technique to develop MA/CNWs resin mixtures followed by characterization of the structural, mechanical, and thermal properties of SIA 3D-printed nanocomposites. Structural and morphological investigations of such nanocomposites reveal the high-level dispersion of CNWs to MA matrix showing the precisely defined nanoscale phase of chitin. We also demonstrated that the addition of small amounts of CNWs can significantly enhance the mechanical (strength, strain at break, and modulus) and thermal properties (Tmax values) of SIA photopolymer MA resins up to an optimum loading of CNWs which is ~1.0 wt% in this work. However, further increasing the content of CNWs to 1.5 wt% reduces the tensile strength, strain at break, and maximum-rate degradation temperatures (T_{max} values) of nanocomposites due to aggregation of excessive fillers in the MA matrix. Lastly, the resulting 3D-printed nanocomposites, even at high filler loading, demonstrate high resolution and accuracy without the need of modifying the settings of a standard SIA 3D-printer.

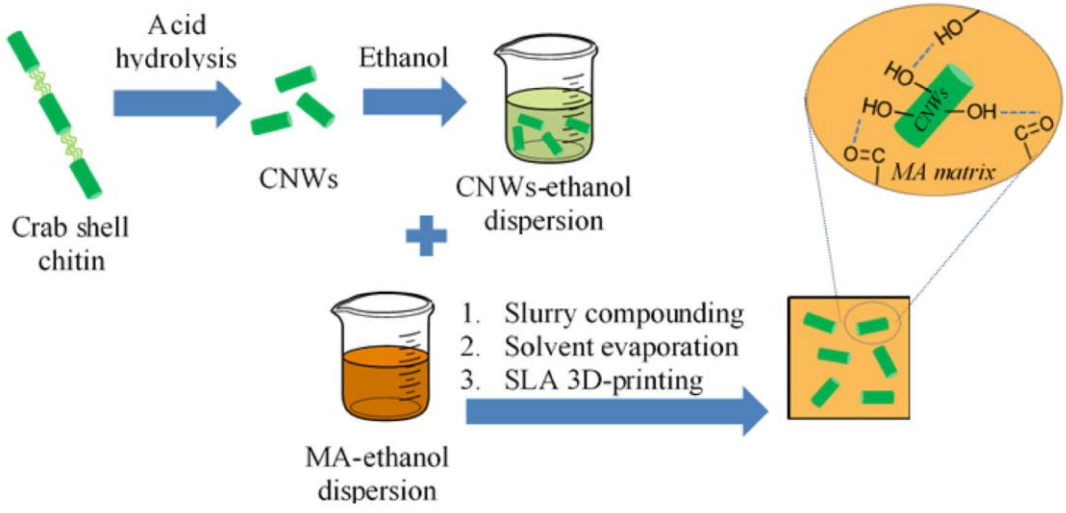

Fig. 1. Preparation of CNWs and MA/CNWs nanocomposites.

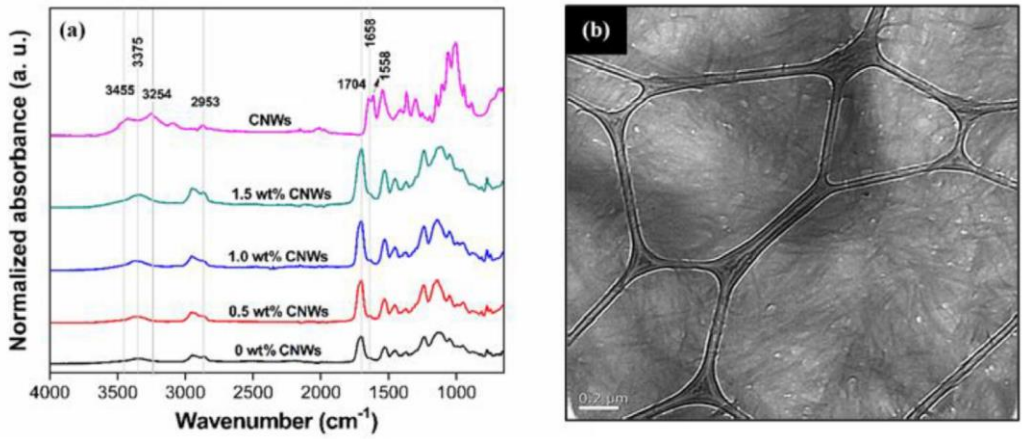

Fig. 2. (a) FTIR spectra of pure CNWs and 3D-printed specimens: pure MA and MA/CNWs nanocomposites with varying CNWs loading and (b) TEM image (200 nm scale) of 3D-printed MA/CNWs nanocomposite containing 1.0 wt% CNWs.

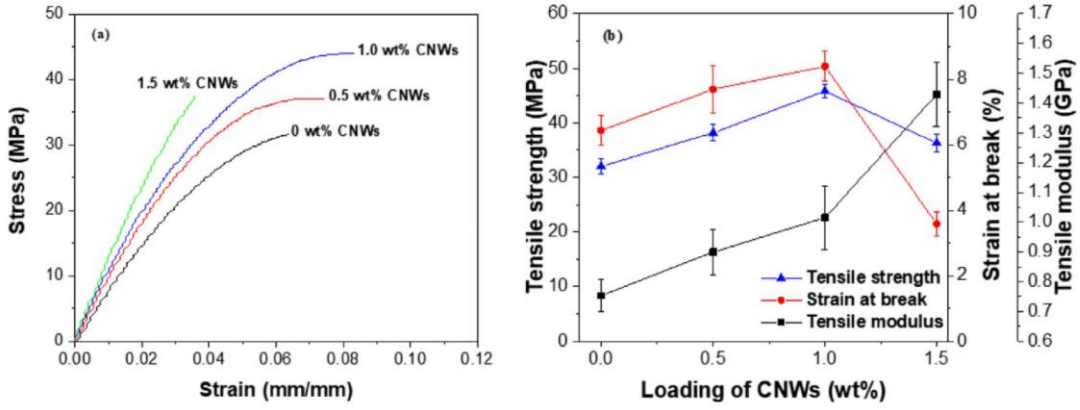

Fig. 3. (a) Stress-strain curves and (b) mechanical properties of JD-printed specimens: pure MA and MA/CNWs nanocomposites with varying CNWs loading.

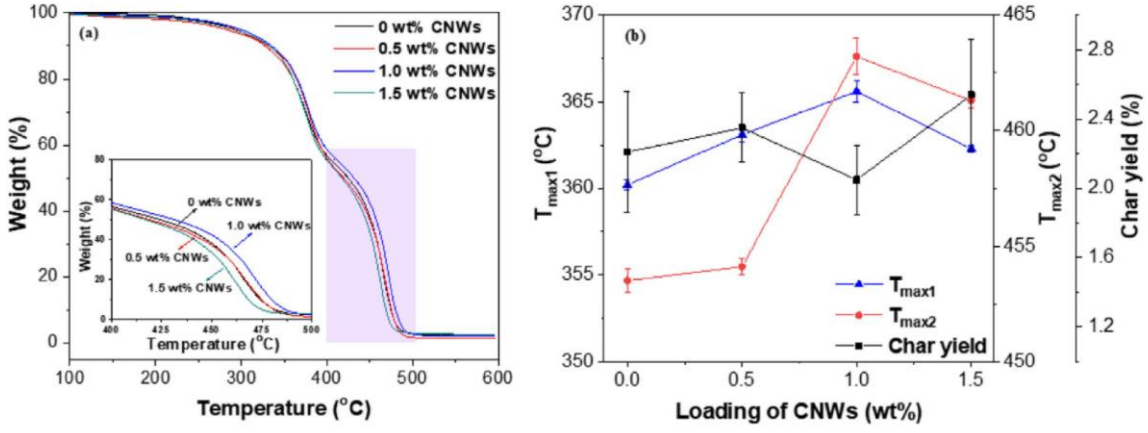

Fig. 4. (a) TGA curves with magnified thermograms from 400 °C to 500 °C and (b) Thermal properties of 3D-printed specimens: pure MA and MA/CNWs nanocomposites with varying CNWs loading.

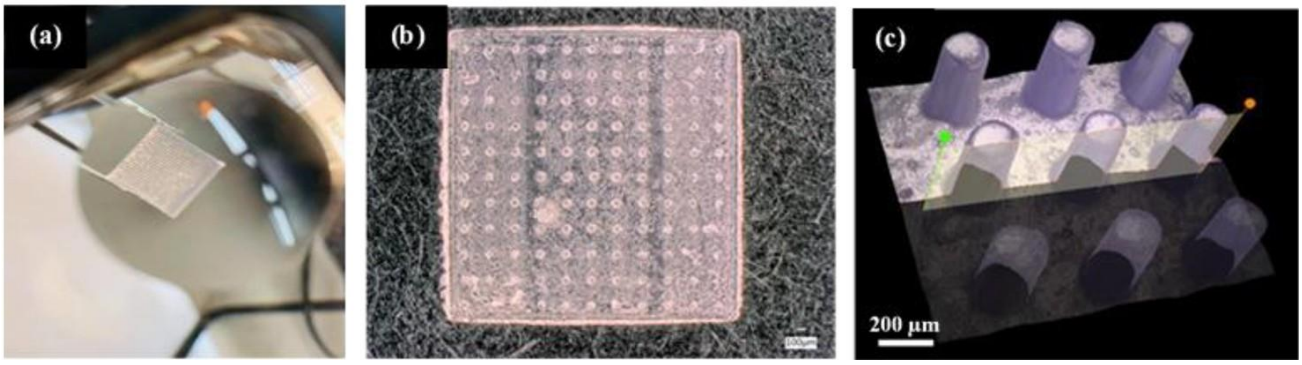

Fig. S. JD-printed micropillars of MA/CNWs nanocomposites containing 1.5 wt% CNWs: (a) optical image, (b) magnified image at 100 µm scale (b),and (c) high-resolution JDreconstruction and surface profilometry.

References

(1) S.C. Ligon, R. Liska, J. Stampfl, M. Gurr , R. Miilhaupt. Polymers for 3D printing and customized additive manufacturing. Chem. Rev. 15 (2017) 10212 - 10290 .
(2) A.C. De Leon, Q, Chen, N.B. Palaganas, j.O.Palaganas.J. Manapat, R.C. Advincula. High performance polymer nanocomposites for additive manufacturing applications, React. Funct. Polym. 103 (2016) 141- 155.
(3) S.A.M. Tofail, E.P. Koumo ulos. A. Bandyopadhyay , S. Bose, L. O'Donoghue. C. Charitidis, Additive manufacturing: scientific and technological challenges. market uptake and opportunities, Mater. Today 21 (2018) 22- 37.
(4) J.R.C. Dizon, A.H. Espera , Q, Chen, R.C. Advincula, Mechanical characterization of 3D- printed polym ers, Addit. Manuf. 20 (2018) 44- 67.
(5) T. Sathish, M.D. Vijayakumar, A.K. Ayyangar, Design and fabrication of industrial components using 3D printing, Mater. Today:. Proc. 5 (2018) 14489 - 14498 .
(6) J.Z. Manapat, Q, Chen, P. Ye, R.C. Advinc ula, JD printing of polymer nanocompositesvia stereolithography, Macromol. Mater. Eng. 302 (2017)1- 13.
(7) B.B. Pajarito, C.A.L. Cayabyab , P.A.C. Costales,j.R. Francisco. Exfoliated graphite / acrylic composite film as hydrophobic coating of 3D-printed polylactic acid surfaces,]. Coat. Technol. Res. 16 (2019) 1133 - 1140 .
(8) X. Feng, Z. Yang, S. Chmely, Q, Wang, S. Wang, Y. Xie, Lignin - coated cellulose nanocrystal filled methacrylate composites prepared via 3D stereolithography printing: Mechanical reinforcement and thermal stabilization, Carbohydr . Polym. 169 (2017) 272- 281.
(9) j.Z. Manapat, j.D. Mangadlao, B.D.B. Tiu, G.C. Tritchler, R.C. Advincula, High- strength stereolithographic 3D printed nanocomposites: graphene oxide metastability, ACS Appl. Mater. Interfaces 9 (2017) 10085- 10093.
(10) j.R.C. Dizon , Q, Chen, A.D. Valina, R.C. Advin cula, Thermo-mechanical and swelling properties of three-dimensional - printed poly (ethylene glycol) diacrylate /silica nanocomposites, MRS Commun. 9 (2019) 209- 217.
(11) H. Korhonen, L.H. Sinh, N.D. Luong, P. Lehtinen, T. Verho,J. Partanen,J. Seppala, Fabrication of graphene -based 3D structures by stereolithography, Phys. Status Solidi A - Appl. Mater. Sci. 213 (2016) 982 - 985 .
(12) N.B. Palaganas. J.D. Mangadlao, A.CC. De Leon, J.O. Palaganas, K.D. Pangilinan, Y.j. Lee, R.C. Advincula, 3D printing of photocurable cellulose nanocrystal composite for fabrication of complex architect ures via stereolithography, ACS Appl. Mater. Interfaces 9 (2017) 34314- 34324.
(13) A. Anitha, S. Sowmya, P.T.S. Kumar, S. Deepthi, K.P. Chennazhi, H. Ehrlich, M. Tsukran, R. Jayaku mar, Chitin and chitosan in selected biomedical applications, Prog. Polym. Sci. 39 (2014) 1644 - 1667 .
(14) A. Morin, A Dufresne, Nanocomposites of chitin whiskers from Riftia tubes and poly(caprolactone), Macromolecules 35 (2002) 2190- 2199.
(15) M.A.S. Anwer,J. Wang, A Guan, H.E. Naguib, Chitin nano-whiskers (CNWs) as a bio-based bio-degradable reinforcement for epoxy: evaluation of the impact of CNWs on the morphological, fracture, mechanical, dynamic mechanical, and thermal characteristics of DGEBA epoxy resin, RSC Adv. 20 (2019) 11063 - 11076 .
(16) K. Wang, L Wang, J. Wu. L Chen, C. He, Preparation of highly exfoliated epoxy /clay nanocomposites by "slurry compounding": process and mechanisms, Langmuir 21 (2005) 3613 - 3618 .
(17) M. Liu, Q, Peng, B. Luo, C. Zhou, The improvement of mechanical performance and water-response of carboxylated SBR by chitin nanocrystals, Eur. Polym. J. 68 (2015) 190- 206.
(18) M. Carve, D. Wlodkowic, 3D-Printed chips: compatibility of additive manufacturing photopolymeric substrata with biological applications, Micromachines. 9 (2018) 91.
(19) B. Redwood. Dimensional accuracy of3D printed parts. 3D Hubs, https: // www. 3dhubs. com/knowledge-base/dimensional-accuracy-3d-printed - parts# variables/ (accessed: Oct 10, 2019).
(20) E. Donath, S. Moya, B. Neu, G.B. Sukhorukov, R. Georgieva, A Voigt, H. Mtihwald, Hollow polymer shells from biological templates: fabrication and potential applications, Chem. A Eur. J. 8 (2002) 5481- 5485.
(21) M. Sadeq Saleh, M. HamidVishkasougheh, H. Zbib, R. Panat, Polycrystalline micropillars by a novel 3-D printing method and their behavior under compressive loads, Ser. Mater. 149 (2018) 144- 149.